Cysteine protease cathepsin B mediates radiation-induced bystander effects

Yu Peng[1,*], **Man Zhang**[1,*], **Lingjun Zheng**[2,3,*], **Qian Liang**[1,*], **Hanzeng Li**[2,*], **Jeng-Ting Chen**[4], **Hongyan Guo**[1], **Sawako Yoshina**[5], **Yu-Zen Chen**[2], **Xiang Zhao**[1], **Xiaoqi Wu**[2,3], **Bin Liu**[3], **Shohei Mitani**[5], **Jau-Song Yu**[4], and **Ding Xue**[1,2]

[1]School of Life Sciences & Collaborative Innovation Center for Diagnosis and Treatment of Infectious Diseases, Tsinghua University, Beijing 100084, China

[2]Department of Molecular, Cellular, and Developmental Biology, University of Colorado, Boulder, CO 80309, USA

[3]College of Food Science, Fujian Agriculture and Forestry University, Fuzhou 350002, Fujian, China

[4]Graduate Institute of Biomedical Sciences, College of Medicine, Chang Gung University and Liver Research Center, Chang Gung Memorial Hospital at Linkou, Taoyuan 333, Taiwan

[5]Department of Physiology, Tokyo Women's Medical University School of Medicine and Core Research for Embryonic Science and Technology (CREST), Japan Science and Technology Agency (JST), Tokyo, 162-8666, Japan

Abstract

Radiation-induced bystander effects (RIBE) refer to a unique process, in which factors released by irradiated cells or tissues exert effects on other parts of the animal not exposed to radiation, causing genomic instability, stress responses, and altered apoptosis or cell proliferation[1–3]. Despite important implications in radioprotection, radiation safety and radiotherapy, the molecular identities of RIBE factors and their mechanisms of action remain elusive. Here we use *C. elegans* as an animal model to study RIBE and have identified a cysteine protease CPR-4, a human cathepsin B homolog, as the first RIBE factor in nematodes. CPR-4 is secreted from animals

irradiated with ultraviolet (UV) or ionizing gamma rays (IR) and is the major factor in the conditioned medium that leads to inhibition of cell death and increased embryonic lethality in unirradiated animals. Moreover, CPR-4 causes these effects and stress response at unexposed sites distal to the irradiated tissue. The activity of CPR-4 is regulated by the p53 homolog *cep-1* in response to radiation and CPR-4 appears to act through the insulin-like growth factor receptor, DAF-2, to exert RIBE. Our study provides critical insights into the elusive RIBE and will facilitate identification of additional RIBE factors and their mechanisms of action.

We tested whether *C. elegans* can serve as an animal model to study RIBE using UV radiation, because UV-induced damage in *C. elegans* is well characterized[4]. Wild-type (N2) animals cultured in the liquid S-Medium were irradiated with 100 J/m^2 UV or sham-irradiated. This UV dosage induced significant embryonic lethality (Extended Data Fig. 1a), which was exacerbated in *cep-1(gk138)* animals defective in the *C. elegans* p53 homolog CEP-1 that is involved in DNA damage repair[4–6]. The medium used to culture irradiated and sham-irradiated animals was called "UV conditioned medium" (UV-CM) and "UV control" (UV-Ctrl), respectively, and used to treat unexposed animals (Fig. 1a). N2 animals treated with UV-CM showed increased embryonic lethality compared with those treated with UV-Ctrl (Extended Data Fig. 1b), indicating that UV-CM contains substances capable of inducing damage in unexposed animals. UV-CM also reduced germ cell death in *ced-1(e1735)* animals, which have many unengulfed apoptotic cells that sensitizes detection of apoptosis, in a manner dependent on the UV dosages (Fig. 1b), reaching maximal death inhibitory activity at 100 J/m^2. These results are consistent with published reports that reduced apoptosis or increased survival of unexposed cells is one of the endpoints of RIBE[3,7–9].

We probed the nature of RIBE factors by treating UV-CM with enzymes that destroy DNA, RNA or proteins. The apoptosis-inhibitory activity in UV-CM was resistant to treatment of DNase or RNase (Extended Data Fig. 2a, b), but obliterated by the Trypsin protease (Fig. 1c), suggesting that the RIBE factors are proteins. UV-CM collected from cell-death defective *ced-3(n2433)* animals, germline-deficient *glp-1(e2141)* animals, or N2 animals fed with dead bacteria retained the death inhibitory activity (Extended Data Fig. 2c–f), indicating that the RIBE factors are unlikely factors generated by bacteria or byproducts of cell death induced by radiation and can be made without the germline.

Using 10 kD molecular weight cut-off filter units, we separated UV-CM into two fractions, one containing proteins likely larger than 10 kD and one with proteins smaller than 10 kD. The RIBE activity appeared in the > 10 kD fraction (Extended Data Fig. 3a), which were resolved on a SDS polyacrylamide gel (Fig. 1d). Protein bands unique to UV-CM were analyzed by mass-spectrometry, from which 19 proteins were identified (Fig. 1e; Extended Data Fig. 4 and Table 1).

We used RNA interference (RNAi) to examine if one of the 19 genes is responsible for RIBE. UV-CM from *cpr-4* RNAi-treated animals displayed a greatly reduced RIBE activity, whereas UV-CM from animals treated with RNAi of other genes retained the RIBE activity (Extended Data Fig. 3b). *cpr-4* encodes a homolog of the mammalian cathepsin B lysosomal protease, which is secreted to act as an extracellular protease[10–12]. Because a deletion

mutation (*tm3718*) in *cpr-4*, which removes one third of the CPR-4 protein (Extended Data Fig. 5a), obliterated the RIBE activity and a single-copy integrated transgene carrying a *cpr-4* genomic fragment with a carboxyl terminal Flag tag (P*cpr-4::cpr-4::flag*) restored RIBE to *cpr-4(tm3718)* animals (Fig. 2a), *cpr-4* is required for this RIBE activity in UV-CM.

We examined whether CPR-4 is secreted into the medium upon UV irradiation. CPR-4::Flag was detected in UV-CM, but not in UV-Ctrl, from P*cpr-4::cpr-4::flag* animals (Fig. 1f). Immunodepletion of CPR-4::Flag from UV-CM of P*cpr-4::cpr-4::flag; cpr-4(tm3718)* animals abolished its RIBE activity (Extended Data Fig. 2g, h), confirming that secreted CPR-4 is the RIBE factor in UV-CM. Because UV-CM from *cep-1(gk138)* animals lost the RIBE activity (Fig. 2a) and UV-CM from *cep-1(gk138); Pcpr-4::cpr-4::flag* animals showed greatly reduced secretion of CPR-4::Flag (Extended Data Fig. 3c), the CPR-4-mediated RIBE are induced through a *cep-1*-dependent mechanism, like some reported p53-dependent RIBE in mammals[3,13].

RIBE often refer to intra-animal bystander effects. We tested if localized UV irradiation (LUI) at the head of an animal might induce bystander effects in other areas of the animal not exposed to radiation (Fig. 3a). Using a stress-response reporter, P*hsp-4::gfp* (*zcIs4*), that also reacts to radiation[14,15], we observed increased GFP expression in multiple unexposed regions of LUI-treated *zcIs4* animals 24 hours post radiation, including strong GFP expression in the posterior region (Fig. 3b, c). This bystander response was strongest in L4 larvae (Fig. 3d), but lost in *cpr-4(tm3718)* and *cep-1(gk138)* mutants (Fig. 3e; Extended Data Fig. 6a), indicating that both *cpr-4* and *cep-1* are required for intra-animal RIBE. LUI also led to increased embryonic lethality in unexposed progeny (Fig. 3a, f) and reduced germ cell death in nonirradiated posterior gonads in a *cpr-4*-dependent manner (Fig. 3a, g), indicating that LUI-induced intra-animal RIBE are similar to inter-animal RIBE induced by UV-CM and that CPR-4 is a bona fide RIBE factor.

CPR-4 and cathepsin B are highly conserved and have identical catalytic residues (Extended Data Fig. 5b), including the active-site Cysteine and a Histidine residue acting as a general base[16]. Using a cathepsin B-specific fluorogenic substrate, z-Arg-Arg-AMC, we detected a cathepsin B-like protease activity in UV-CM, but not in UV-Ctrl, from N2 animals (Fig. 2b). This activity was absent in UV-CM from *cpr-4(tm3718)* animals, greatly reduced in UV-CM from *cep-1(gk138)* animals, but restored in P*cpr-4::cpr-4::flag; cpr-4(tm3718)* animals, confirming that CPR-4 confers this cathepsin B-like activity in UV-CM through a *cep-1*-dependent mechanism.

We tested if recombinant CPR-4 recapitulated the RIBE activity. A truncated CPR-4 lacking its signal peptide (residues 1-15), tCPR-4, exhibited a similar protease activity to that of recombinant human cathepsin B (rhCTSB)(Extended Data Fig. 3d). Mutations altering the conserved catalytic residues, C109A and H281A, abolished the protease activity of tCPR-4 (Fig. 2c), whereas a mutation (N301A) changing a non-catalytic residue did not affect tCPR-4 protease activity[16]. Like UV-CM from N2 animals, tCPR-4, tCPR-4(N301A), and rhCTSB reduced germ cell corpses (Fig. 2d; Extended Data Fig. 3e) and increased embryonic lethality (Extended Data Fig. 1c), whereas tCPR-4(H281A) and tCPR-4(C109A) failed to do so, indicating that the CPR-4 protease activity is critical for its RIBE activities.

We tested conditioned medium from animals irradiated by a different radiation source, ionizing radiation (IR-CM), and its sham-irradiated control (IR-Ctrl). IR-CM from N2 or P*cpr-4::cpr-4::flag; cpr-4(tm3718)* animals reduced germ cell corpses in *ced-1(e1735)* animals, whereas IR-CM from *cpr-4(tm3718)* or *cep-1(gk138)* animals had no such activity (Fig. 2e). Likewise, IR-CM, but not IR-Ctrl, from N2 animals caused increased embryonic lethality (Extended Data Fig. 1b) and contained a cathepsin B-like activity that was lost in IR-CM from *cpr-4(tm3718)* or *cep-1(gk138)* animals, but restored in P*cpr-4::cpr-4::flag; cpr-4(tm3718)* animals (Fig. 2f). Moreover, secreted CPR-4::Flag was detected in IR-CM, but not in IR-Ctrl, from P*cpr-4::cpr-4::flag* animals (Fig. 2g). Therefore, CPR-4 is a shared RIBE factor induced by different radiation sources.

Using quantitative RT-PCR analysis, we found that the transcription of the *cpr-4* gene in N2 animals was elevated by approximately 1.6 fold after UV or IR irradiation, compared with sham-irradiated controls (Fig. 2h). By contrast, *cpr-4* transcription in *cep-1(gk138)* animals was not altered by either radiation. These results indicate that ionizing and non-ionizing radiation increases *cpr-4* transcription through a CEP-1-dependent mechanism, leading to synthesis of more CPR-4 proteins and enhanced secretion of CPR-4.

Using a single-copy insertion transgene carrying a *cpr-4* transcriptional fusion with green fluorescent protein (GFP) and a nuclear localization signal (P*cpr-4::nls::gfp*), we examined when and where *cpr-4* is expressed. In N2 animals, NLS::GFP expression was not detected in embryos, was observed in the intestine of early stage larvae (L1 to L3), peaked at the L4 larval stage, and declined when animals entered the adulthood (Extended Data Fig. 7a–h, j). Similar spatiotemporal NLS::GFP expression patterns were observed in *cep-1(gk138);* P*cpr-4::nls::gfp* animals (Extended Data Fig. 7i, j). When irradiated with UV, N2 animals, but not *cep-1(gk138)* animals carrying P*cpr-4::nls::gfp*, showed elevated NLS::GFP expression (Extended Data Fig. 7k), confirming that radiation induces increased *cpr-4* transcription through a *cep-1*-dependent mechanism.

To investigate the effects of secreted CPR-4 *in vivo*, we generated transgenic P*myo-2*::CPR-4::mCherry animals expressing CPR-4::mCherry specifically in *C. elegans* pharynx under the control of the *myo-2* gene promoter (Extended Data Fig. 8a). As expected of a secreted protein, CPR-4::mCherry was made in and secreted from the pharynx and taken up by cells in the whole body, including the phagocytic coelomocytes (arrowheads, Extended Data Fig. 8a). Removal of the CPR-4 signal peptide blocked tCPR-4::mCherry secretion from the pharynx in transgenic animals (Extended Data Fig. 8b). Like UV-CM, IR-CM or LUI treatment, pharyngeal expression of CPR-4::mCherry increased embryonic lethality, decreased germ cell death, and in addition, caused substantial larval arrest (Extended Data Fig. 8c, d), which were not seen or greatly attenuated in animals expressing tCPR-4::mCherry or catalytically inactive CPR-4::mCherry proteins. These results from ectopic expression of CPR-4 provide further evidence to support a long-range signaling role of CPR-4 as a RIBE factor.

Given the various RIBE effects mediated by CPR-4, we investigated how CPR-4 influences unexposed cells or animals through examining genes that affect multiple cellular processes. The *daf-2* gene, which encodes a *C. elegans* ortholog of the human insulin/IGF receptor and

regulates multiple signaling pathways[17–20], was examined, as reduced *daf-2* activity increases life span and stress resistance[17,18] and decreases germ, muscle and neuronal cell death induced by genotoxic and hypoxic stresses[19,20]. Similarly, reduced *daf-2* function by a temperature-sensitive mutation (*e1370*) decreased physiological germ cell death (Fig. 4a). Interestingly, purified tCPR-4 did not further reduce germ cell death in the *ced-1(e1735); daf-2(e1370)* mutant (Fig. 4a), suggesting that tCPR-4 and *daf-2* act in the same pathway to affect germ cell death. Moreover, tCPR-4 did not reduce germ cell death in *ced-1(e1735); pdk-1(sa680)* animals, which are defective in the PDK-1 kinase, a key downstream signaling component of DAF-2[21], but could do so in *daf-16(mu86) ced-1(e1735)* animals, which lack DAF-16[22,23], one of the major transcription factors acting downstream of DAF-2 (Extended Data Fig. 6b). We observed similar results using the LUI assays wherein inactivation of *daf-2* and *pdk-1*, but not *daf-16,* prevented increased GFP expression from P*hsp-4::gfp* in the posterior unexposed regions (Fig. 3e and Extended Data Fig. 6a) and loss of *daf-2* blocked increased embryonic lethality and reduced germ cell death in unexposed tissues (Fig. 3f, g). Because loss of *daf-2* did not seem to affect the secretion of CPR-4 into UV-CM or the apoptosis-inhibitory activity of UV-CM (Extended Data Fig. 6c, d), these results support a model wherein the secreted CPR-4 acts through the DAF-2 insulin/IGF receptor and the PDK-1 kinase, but not the DAF-16 transcription factor, to exert RIBE in unexposed cells.

Because *daf-2* also affects germ cell proliferation[24,25], we examined if tCPR-4 treatment alters germ cell proliferation by scoring the number of nuclei in the germline mitotic region[24]. tCPR-4 treatment of N2 animals resulted in more germ cell nuclei and more metaphase nuclei in the mitotic zone (Fig. 4b), suggesting a stimulating effect. Reduced *daf-2* activity or loss of *cep-1* blocked increased germ cell proliferation induced by tCPR-4 (Fig. 4b and Extended Data Fig. 6e), indicating that tCPR-4 promotes germ cell proliferation through DAF-2 and CEP-1.

RIBE is a major factor in determining the efficacy and success of radiotherapy in cancer treatment[2,26,27], not only because it affects and causes damage in nonirradiated cells, but also because it can affect irradiated cells through paracrine signaling. Thus, identification of RIBE factors is a fundamental issue in cancer radiotherapy and radioprotection[1]. Using the *C. elegans* animal model, we identify CPR-4, a cathepsin B homolog, as the major RIBE factor that induces multiple, typical RIBE effects[1,27], including apoptosis inhibition and increased cell proliferation, lethality, and stress response. In mammals, cathepsin B is secreted from lysosomes to exert extracellular activities, including regulation of apoptosis, and plays roles in neoplastic and inflammatory disease states[28,29]. Recent studies show that extracellular cathepsin B enhances breast cancer resistance to drug-induced apoptosis during chemotherapy[30], which is consistent with our observations in *C. elegans*. We show that radiation increases *cpr-4* transcription and CPR-4 protein production and secretion in *C. elegans* through a p53/CEP-1-dependent mechanism. The secreted CPR-4 then induces multiple RIBE responses, either directly or indirectly, through regulating the activity of the DAF-2 insulin/IGF receptor that is critical for multiple conserved signaling pathways, from aging, stress response, metabolism, to apoptosis[17,18]. Therefore, our study provides critical insights into the elusive RIBE phenomenon, not only on how it is generated and what the RIBE factor is, but also on how the RIBE factor impacts non-irradiated cells. This *C. elegans*

model will facilitate identification of additional RIBE factors and underlying mechanisms in worms and in other organisms.

Methods

Strains and culture conditions

We cultured *C. elegans* strains at 20°C using standard procedures[31], unless otherwise noticed. We used the N2 Bristol strain as the wild-type strain. The following stains were used in the genetic analyses: LGI, *cep-1(gk138)*, *daf-16(mu86)*, *ced-1(e1735)*; LGII, single copy insertion of P*cpr-4::cpr-4::flag*[32], single copy insertion of P*cpr-4::nls::gfp*; LGIII, *daf-2(e1370)*, *glp-1(e2141)*; LGV, *cpr-4(tm3718)*, *zcIs4* (P*hsp-4::gfp*); LGX, *pdk-1(sa680)*. Each single-copy insertion transgene was backcrossed at least four times with N2 animals before being used.

Irradiation

Adult animals grown on Nematode Growth Media (NGM) plates or in plastic tubes with liquid culture media were irradiated at room temperature using a UV-cross-linker or a Co^{60} radiation source. The dosage of UV irradiation was 100 J/m². The dosage of Co^{60} irradiation was 500 Gy at a dosage rate approximately 33.3 Gy/minute. Plates were returned to 20°C incubators immediately after irradiation. Plastic tubes were placed in a 20°C shaker after irradiation to generate conditioned medium. Sham-irradiated controls were used in all irradiation experiments.

Generation of conditioned medium from irradiated animals

C. elegans animals close to starving were washed off from three NGM plates (6 cm in diameter) and cultured for six days in 250 mL of S-Medium (100 mM NaCl, 5.8 mM K_2HPO_4, 44 mM KH_2PO_4, 0.013 mM cholesterol, 1 mM citric acid monohydrate, 9 mM tri-potassium citrate monohydrate, 0.05 mM disodium EDTA, 0.025 mM $FeSO_4$, 0.01 mM $MnCl_2$, 0.01 mM $ZnSO_4$, 0.001 mM $CuSO_4$, 1.5 mM $CaCl_2$, 3 mM $MgSO_4$, 0.13 mM ampicillin, 0.007 mM streptomycin sulfate, 0.16 mM neomycin sulfate, and 0.02 mM Nystatin) using plentiful *Escherichia coli* strain HB101 as a food source. The animals were harvested by precipitation at 4°C for 10 minutes, which were mostly adults, and washed with S-Medium three times. We adjusted the animal density to approximately 2 animals/μL in S-Medium, transferred them to a quartz plate (with lid), and irradiated them using UV with the desired dosages or sham-irradiated. For IR irradiation, animals at the same density were transferred to 15 mL Corning centrifuge tubes and irradiated using 500 Gy IR or sham-irradiated. The irradiated or sham-irradiated animals were washed with fresh S-Medium, transferred to 15 mL Corning centrifuge tubes in 6 mL S-Medium supplemented with the HB101 bacteria, and grown in a 20°C shaker for 24 hours with constant 200 rpm shaking. After that, we removed the animals and bacteria by centrifugation at 3000 rpm for 10min and filtrated the medium with a 0.22 μm filter unit to obtain conditioned medium. The conditioned medium was then concentrated by passing through a 10 kD ultrafiltration tube (Amicon Ultra-15, Millipore) and adjusted to 0.1 μg/μL total protein concentration using S-Medium. To generate UV-CM and UV-Ctrl from P*cpr-4::cpr-4::flag; daf-2(e1730); cpr-4(tm3718)* animals, starved plates containing the animals were chunked to 300 new

NGM plates, which were placed at 20°C for 2 days before being shifted to 25°C for one more day. UV-irradiated or sham-irradiated animals were grown in a 25°C shaker for 24 hours to obtain UV-CM and UV-Ctrl.

Localized irradiation in *C. elegans*

C. elegans L4 larvae were mounted on an agarose pad (2%) with 10 nM Sodium Azide and irradiated at the head region using a Nikon A1 laser scanning confocal on an inverted Ti-E microscope with a 40x/0.9 NA Plan Apo Lambda objective lens. At installation, the 405 nm laser power, which is very close to the wavelength of UV, was measured at 23.32 mW at the fiber. Irradiation was performed using 60% 405 nm laser power at 512×512 with a pixel size of 0.58 micron $\times$ 0.58 micron for 2.2 microseconds/pixel. Using a Thor labs power meter (PM100D) and photosensor (S140C), we measured the power at the sample plane to be approximately 0.25–0.30 mW. This corresponds to approximately $0.75 - 0.89$ mW/micron^2 at the sample. For sham-irradiation controls, a region slightly away from the animal on the agarose pad was irradiated. After irradiation, the animals were immediately rescued from the agarose pad and transferred to a regular NGM plate to recover at 20°C for 24 hours or at 25°C for 20 hours (embryonic lethality assays) before being assayed for intra-animal bystander effects. Three assays were conducted to monitor intra-animal bystander effects in unexposed areas. They are germ cell corpse assays in the posterior gonads, embryonic lethality assays of the F1 progeny of irradiated animals, and P*hsp-4::gfp* stress response assays in the posterior region. For P*hsp-4::gfp* stress response assays, experiments using the *daf-2(e1370ts)* strains and corresponding control strains were performed at 25°C after LUI. For the embryonic lethality assays, after 20-hour recovery at 25°C, irradiated or sham-irradiated animals were placed on NGM plates to lay eggs for 4 hours at 25°C and then transferred to new NGM plates. After two more transfers, the animals were discarded. The number of eggs that did not hatch (scored as dead eggs) and the number of eggs that developed into larvae were scored and used to determine the rate of embryonic lethality.

Formaldehyde-treated bacteria as the food source

HB101 bacteria were treated with 3.7% formaldehyde for 10 minutes, washed three times with S-medium, and collected by centrifugation. The death of bacteria was verified by spreading them on a plate with no antibiotics and observing no bacterial colony. The bacterial pellets were added to S-medium to grow worms.

RNA interference (RNAi) experiments

RNAi experiments were performed using a bacterial feeding protocol[33]. HT115 bacteria transformed with the pPD129.36-*cpr-4* or the pPD129.36 plasmid were used in *cpr-4* RNAi and control RNAi experiments, respectively. Bacterial clones used in other RNAi experiments are from an RNAi library purchased from ThermoFisher. To perform RNAi experiments in liquid culture, three NGM plates with RNAi bacteria were used to feed 30 larval stage 4 (L4) N2 animals until the plates were almost starved. We then washed the animals off the plates and transferred them to glass flasks with 250 mL of S-Medium containing 0.5 mM Isopropyl β-D-1-thiogalactopyranoside (IPTG) and the RNAi bacteria and grew them for one more generation. The procedure to obtain conditioned medium is similar to that described above.

Growing *C. elegans* animals in 96-well plates

HB101 bacteria were mixed with 100 μL conditioned medium (0.1 μg/μL) or 100 μL S-Medium containing 2.8 μM of recombinant tCPR-4 proteins (wild-type or mutant) or 0.27 μM recombinant human cathepsin B in a 96-well plate. Approximately 60 L4 larvae were transferred into each well of the plate. After being cultured in liquid media for 48 hours, these animals were scored for the numbers of germ cell corpses and mitotic nuclei.

Enzyme treatment of conditioned medium

The nature of the RIBE factor was analyzed by treating conditioned medium with different enzymes. 1 μL DNase (1 Unit/μL, QIAGEN), 1 μL RNase (100 μg/μL, QIAGEN) or 1 μL Trypsin (5μg/μL, Sigma) was mixed with 100 μL conditioned medium for 1 hour at 30°C. The treated or untreated conditioned medium was then used to culture *ced-1(e1735)* animals for 48 hours at 20°C in a 96-well plate.

Quantification of germ cell corpses

L4 animals were cultured in liquid media in a 96-well plate as described above. After 48 hours, they were transferred to NGM plates and allowed to recover for 1 hour at 20°C. The animals were then anesthetized by 20 mM NaN_3, mounted onto 2% agar pad, and scored under Nomarski optics. For transgenic animals expressing CPR-4 in the pharynx, L4 animals were grown on NGM plates for 24 hours at 20°C before they were scored for germ cell corpses. Only the posterior arms of intact gonads were scored. Blind tests were carried out in all germ cell corpse quantification experiments.

Quantification of mitotic nuclei

L4 animals treated with 2.8 μM of purified tCPR-4 proteins in liquid culture for 48 hours were transferred to NGM plates and allowed to recover for 1 hour at 20°C. They were then dissected to expose their gonads following the protocol described previously[24]. Dissected gonads were fixed and stained with DAPI[34]. The number of germ nuclei and the number of metaphase nuclei in the mitotic zone of each gonad were scored using a Zeiss Nomarski microscope with a DAPI filter[24].

Quantification of the expression levels of *cpr-4* through the GFP reporter

A single-copy insertion of the P*cpr-4::nls::gfp* transgene[32] was used to determine the expression levels of *cpr-4* before and after irradiation. Middle stage L4 P*cpr-4::nls::gfp* and *cep-1(gk138);* P*cpr-4::nls::gfp* larvae were irradiated with 100 J/m^{2} UV and allowed to recover for 2 hours at 20°C before imaging. The GFP expression patterns of the animals were recorded by capturing images under Nomarski optics. The exposure times of all images were fixed at 100 ms. The intensity of GFP fluorescence in each animal was quantified using the Image J software (NIH). The expression levels of *cpr-4* at different developmental stages (embryos, L1, L2, L3, L4 larvae, adults at 24 hours and 48 hours post L4) without irradiation were determined using the same method.

Embryonic lethality and larval arrest assays

For embryonic lethality assays caused by direct irradiation, after irradiated with 100 J/m^2 UV or 500 Gy gamma ray, gravid adults were placed on NGM plates to lay eggs for 4 hours at 25°C and then removed from the plates. For embryonic lethality assays in liquid media, L4 larvae were cultured in conditioned medium or S-Medium containing the purified proteins at 20°C for 48 hours, transferred to fresh NGM plates from the liquid media, and allowed to lay eggs for 4 hours at 25°C, before the adult animals were removed. For embryonic lethality assays in transgenic animals expressing CPR-4 in the pharynx, transgenic gravid adults at 24 hours post L4 were placed on NGM plates to lay eggs for 4 hours at 25°C and then removed from the plates. In all cases, after 24 hours at 25°C on NGM plates, the number of eggs that did not hatch (scored as dead eggs) and the number of eggs that developed into larvae were scored and used to determine the rate of embryonic lethality.

For the larval arrest assays, gravid transgenic adults were placed on NGM plates, control RNAi plates, or *cpr-4* RNAi plates to lay eggs for 4 hours at 25°C. The number of transgenic larvae that hatched out was scored under the fluorescence stereoscope before the plates were returned to the 20°C incubator. After 3 days, the number of transgenic animals that did not enter the adult stages was scored and used to determine the rate of larval arrest.

Molecular biology

Full-length *cpr-4* cDNA was amplified by polymerase chain reaction (PCR) from a *C. elegans* cDNA library. The signal peptide of CPR-4 is predicted using the SignalP 3.0 Server[35]. To construct the pGEX4T-2-tCPR-4 plasmid, a *cpr-4* cDNA fragment encoding residues 16-336 was PCR amplified from the full-length *cpr-4* cDNA clone and subcloned into a modified pGEX4T-2 vector through its *NdeI* and *XhoI* sites, which has a PreScission Protease cleavage site LEVLFQGP inserted right after the GST coding sequence. To make the pGEX4T-2-tCPR-4(C109A), pGEX4T-2-tCPR-4(H281A) and pGEX4T-2-tCPR-4(N301A) vectors, two-step PCR was used to generate the tCPR-4 cDNA fragment carrying the indicated mutation, which was subcloned into the same modified pGEX4T-2 vector through its *NdeI* and *XhoI* sites. To construct P*myo-2*::CPR-4::mCherry, P*myo-2*::tCPR-4::mCherry, P*myo-2*::CPR-4(C109A)::mCherry, P*myo-2*::CPR-4(H281A)::mCherry, and P*myo-2*::CPR-4(N301A)::mCherry expression vectors, the cDNA fragments encoding full-length CPR-4(C109A), CPR-4 (H281A) and CPR-4 (N301A) were first generated using a two-step PCR method. The DNA fragments encoding CPR-4::mCherry, tCPR-4::mCherry, CPR-4(C109A)::mCherry, CPR-4(H281A)::mCherry and CPR-4(N301A)::mCherry were similarly PCR amplified and subcloned into a modified pCFJ90 vector (Addgene) through its *NheI* sites.

To make the plasmid pCFJ151-P*cpr-4*::*cpr-4*::*flag* for generating the single copy integrated transgene, a *cpr-4* genomic fragment (P*cpr-4*::*cpr-4*::*utr*), containing 4018 bp of the *cpr-4* promoter sequence, 1196 bp of the *cpr-4* genomic coding sequence, and 2267 bp of the *cpr-4* 3′ untranslated region (UTR), was excised from a fosmid WRM0619bH11 through digestion with *PmlI* and *BssHII* and then subcloned into a modified pCFJ151 plasmid through its *BssHII* site and a blunted *AvrII* site. This P*cpr-4*::*cpr-4*::*utr* genomic fragment

was then excised from the plasmid through *AflII* and *NheI* digestion and subcloned into a plasmid pSL1190 through its *AflII* and *NheI* sites. A Flag tag (DYKDDDDK) was inserted immediately after the *cpr-4* coding region through the QuickChange method. The modified P*cpr-4::cpr-4::flag::utr* genomic fragment was subcloned back to pCFJ151 through its *AflII* and *NheI* sites to obtain the plasmid pCFJ151-P*cpr-4::cpr-4::flag*.

To construct the plasmid pSL1190-P*cpr-4::nls::gfp* for single copy insertion, a 4114 bp fragment containing the *cpr-4* promoter and the first 58 bp of the *cpr-4* coding region, a 1767 bp fragment containing the NLS::GFP coding sequence and the *unc-54* 3′ UTR, a 1337 bp upstream homologous recombination fragment of the LGII Mos I site (ttTi5605) and a 1418 bp downstream homologous recombination fragment of the LGII MosI site were ligated into the pSL1190 plasmid backbone through its *PstI* and *BamHI* sites using the Gibson ligation method.

To construct the plasmid for *cpr-4* RNAi, full-length *cpr-4* cDNA fragment was PCR amplified and subcloned into the pPD129.36 vector through its *Nhe I* and *Xho I* sites. All clones generated were confirmed by DNA sequencing.

Transgenic animals

Transgenic animals were generated using the standard protocol[36]. P*myo-2::*CPR-4::mCherry, P*myo-2::*tCPR-4::mCherry, P*myo-2::*CPR-4(C109A)::mCherry, P*myo-2::*CPR-4(H281A)::mCherry, or P*myo-2::*CPR-4(N301A)::mCherry was injected into *ced-1(e1735); cpr-4(tm3718)* animals at 20 ng/μL (for quantification of germ cell corpses) or 2 ng/μL (for embryonic lethality and larval arrest assays) along with the pTG96 plasmid (at 20 ng/μL) as a co-injection marker. The pTG96 plasmid contains a *sur-5::gfp* translational fusion that is expressed in many cells and in most developmental stages[37]. Single-copy insertion P*cpr-4::cpr-4::flag* transgene and P*cpr-4::nls::gfp* transgene were generated using a method described previously[32].

Immunoblotting detection of secreted CPR-4::Flag

Conditioned medium derived from irradiated N2, P*cpr-4::cpr-4::flag*, P*cpr-4::cpr-4::flag; cpr-4(tm3178)*, *cep-1(gk138)*; P*cpr-4::cpr-4::flag*, or P*cpr-4::cpr-4::flag; daf-2(e1370);cpr-4(tm3178)* animals was concentrated using a 10 kD molecular weight cut-off (MWCO) centrifugal filter column (1 μg/μL final protein concentration). Concentrated conditioned media were resolved on a 12% SDS polyacrylamide gel (SDS-PAGE) and transferred to a PVDF membrane. Secreted CPR-4::Flag was detected using a monoclonal antibody to the Flag tag (Sigma, catalog number F3165, 1:2000 dilution) and a goat-anti-mouse secondary antibody conjugated with horseradish peroxidase (HRP, Bio-Rad, catalog number 1705047, 1:5000 dilution).

CPR-4::Flag depletion

UV-CM or UV-Ctrl derived from P*cpr-4::cpr-4::flag; cpr-4(tm3718)* animals were incubated with 20 μL bed volume anti-Flag M2 affinity gel (Sigma, catalog number A2220) overnight at 4°C on a rotary shaker. The anti-Flag beads were spun down by centrifugation at 10,000

rpm for 2 minutes and the supernatant was collected and used as anti-Flag-depleted conditioned medium.

Protein expression and purification

tCPR-4 or mutant tCPR-4 proteins (C109A, H281A, or N301A) were expressed in the *Escherichia coli* strain BL21(DE3) with a N-terminal GST tag and a C-terminal His_6-tag. The soluble fraction of bacteria was purified using a Glutathione Sepharose column (GE Healthcare, catalog number 17-0756-01) and cleaved by the PreScission Protease at room temperature for 2 hours to remove the GST tag. The proteins were then affinity purified using a Ni^{2+} Sepharose column (GE Healthcare, catalog number 17-5268-01) and eluted from the column with 250 mM imidazole. Purified proteins were concentrated using 5 kD MWCO centrifugal filter units to approximately 200 ng/μL final concentration and dialyzed twice using a dialysis buffer containing 25 mM Tris-HCl (pH 8.0), 100 mM NaCl, 1mM DTT and 10%(v/v) glycerol at 4°C for 4~6 hours with magnetic stirring. Insoluble aggregates after dialysis were removed by high-speed centrifugation. The proteins were then diluted to 100 ng/μL final concentration with the dialysis buffer and stored at -80°C in aliquots. The concentrations of purified proteins were determined by anti-His_6 immunoblotting, using tCPR-4-His_6 with a known concentration as a normalizing control.

Mass spectroscopy analysis

The protein bands of interests excised from the silver-stained gels were destained by 1% potassium ferricyanide and 1.6% sodium thiosulfate, subjected to reduction and alkylation by 10 mM DTT and 55 mM iodoacetamide in 25 mM NH_4HCO_3, and then in-gel digested with trypsin (20 μg/mL in 25 mM NH_4HCO_3) at 37 °C for 16 hours. The reaction products were analyzed with liquid chromatography tandem mass spectrometry (LC-MS/MS) using a linear ion trap mass spectrometer (LTQ-Orbitrap, Thermo Fisher). Samples were loaded across a trap column (Zorbax 300SB-C18, 0.3×5 mm, Agilent Technologies) and peptides were separated on an analytical column (capillary RP18 column, Synergy hydro-RP, 2.5 μm, 0.075×100 mm, packed in house) with a gradient of 2–95% HPLC buffer (99.9% acetonitrile containing 0.1% formic acid) in 75 minutes. For the MS analysis, we used a data-dependent procedure that alternated between one MS scan and six MS/MS scans for the six most abundant precursor ions. The resulting spectra were used in searches of the sprot_20140416 database (selected for *Caenorhabditis elegans*, 3466 entries) assuming the digestion enzyme trypsin. The MASCOT search engine (http://www.matrixscience.com; v. 2.2.2 Matrix Science) was used, allowing two missing cleavage sites with charge states from 2^+ to 3^+. The parent ion mass tolerance was set to 10 ppm and the fragment ion mass tolerance was set to 0.5 Da for both fix modification (carbamidomethylation of cysteine) and variable modifications (acetylation at protein N-terminal, oxidation of methionine, and Gln change to pyro-Glu). The DAT files produced by Mascot Daemon were subjected to search using Scaffold 3 search engine (v.3.06.01; http://www.proteomesoftware.com). Protein identification is accepted if protein probability is > 95%, containing at least two peptides with peptide prophet algorithm probability > 95%.

Measurement of protease activity *in vitro*

The CPR-4 enzymatic assays were performed following the method described previously with some modifications[38]. The cathepsin B-specific fluorogenic substrate, Z-Arg-Arg-7-amido-4-methylcoumarin hydrochloride (z-Arg-Arg-AMC; Peptanova, catalog number 88937-61-5), was dissolved in $2 \times$ reaction buffer, containing 25 mM Tris-HCl (pH 8.0), 100 mM NaCl, 10% (v/v) Glycerol, 0.8 mM Sodium Acetate (pH6.0), and 8 mM EDTA. For the assays, 10 μL of proteins (100 ng/μL) or 10 μL of conditioned medium (100 ng/μL) were incubated with 10 μL of 20 μM z-Arg-Arg-AMC at 25°C for 10 minutes before measuring the luminescence. Enzymatic activities were determined as the mean velocities at 25°C in a dual luminescence fluorometer EnVision (Perkin-Elmer) at an excitation wavelength of 380 nm and an emission wavelength of 460 nm, and expressed as relative intensity in kilo relative fluorescence unit (kRFU). Recombinant human cathepsin B (rhCTSB; Sino Biological Inc., catalog number 10483-H08H-10) was dissolved in a buffer recommended by the manufacturer [25 mM Tris-HCl (pH 8.0), 100 mM NaCl, 10% (v/v) glycerol, 5mM DTT, and 0.1% Triton-X]. The buffer control unique to the CPR-4 proteins or the rhCTSB protein, or the sham-irradiated conditioned medium, was also measured using the same procedures. S-Medium was used in each experiment as the background control.

## Quantitative RT-PCR analysis of the *cpr-4* transcriptional levels

N2 and *cep-1(gk138)* L4 larvae were transferred to fresh NGM plates and cultured at 20°C for 24 hours. Two hours after they were subjected to 100 J/m² UV or 500 Gy gamma ray irradiation or sham-irradiation, they were lysed for total RNA extraction using the RNAiso kit (TaKaRa, catalog number 9108). Isolated total RNAs were used as templates in reverse transcription (RT) using the ImProm-II™ Reverse Transcription System (Promega, catalog number A3800) to obtain the first strand cDNA according to manufacturer's instructions.

Quantitative PCR analysis was carried out using a Bio-Rad CFX96 Touch real-time PCR detection system using the iTaq™ SYBR® Green Supermix with ROX (Bio-Rad, catalog number 1725151). Each PCR reaction contained 12.5 μL of the Bio-Rad supermix solution, 50 nM of forward and reverse primers, and 5 μL cDNA (150 ng/μL) in a final volume of 25 μL. Amplifications were performed in real-time PCR tubes (Bio-Rad, catalog number TLS0851) placed in the 96-well of the real-time PCR detection system. The cycling conditions were as follows: 95°C for 3 minutes for denaturation, followed by 50 cycles of 20 seconds at 95°C, 30 seconds at 60°C, and 20 seconds at 72°C. Melting curve analysis was performed after the final cycle to examine the specificity of primers in each reaction. PCR reactions were run in triplicate and three independent experiments were performed. The transcription of *pmp-3* was used as the internal reference due to its unusually stable expression levels in adults[39]. The data were analyzed by the Livak method. The primers to detect *cpr-4* are 5′-TCGGAAAGAAGGTCTCCCAGAT-3′ (forward primer) and 5′-GGTAGAAGTCCTCGTAGACAGTGAAT-3′ (reverse primer). The primers to detect *pmp-3* are 5′-GTTCCCGTGTTCATCACTCAT-3′ (forward primer) and 5′-ACACCGTCGAGAAGCTGTAGA-3′ (reverse primer).

Data availability

The uncropped versions of the blots are provided as Supplementary Figure 1 in Supplementary Information (SI). The majority of the raw data for the figures and tables presented in this paper are also provided in SI. The other data that support the findings of this study are available from the corresponding author upon reasonable request.

Extended Data
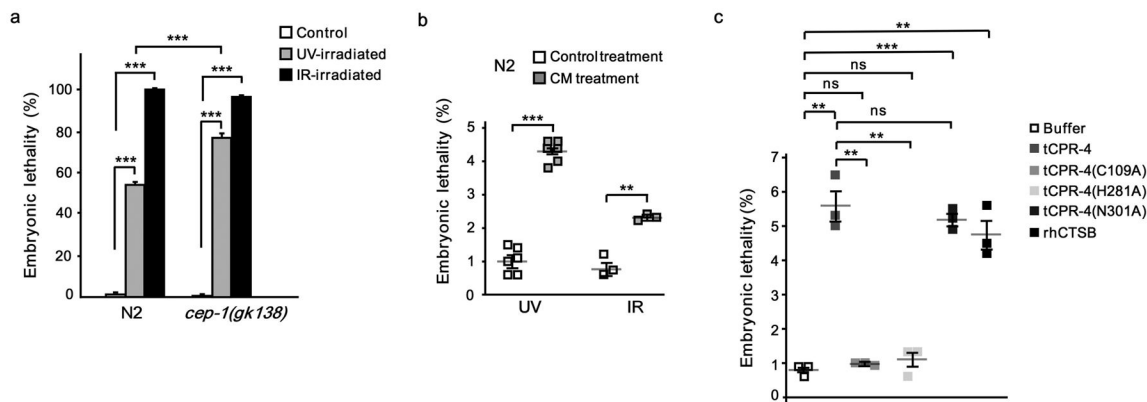
Extended Data Figure 1. Conditioned medium generated from UV or ionizing irradiation (IR) and purified tCPR-4 proteins cause embryonic lethality

a, The embryonic lethality rate of wild type (N2) or *cep-1(gk138)* animals after 100 J/m^2 UV irradiation or 500 Gy IR compared with sham-irradiation controls. **b,** N2 animals were used to generate UV-CM, UV-control, IR-CM and IR-control, which were used to treat unexposed N2 animals in the embryonic lethality assays (Methods). **c,** 2.8 μM of recombinant tCPR-4 proteins (wild-type or mutant), 0.27 μM recombinant human Cathepsin B (rhCTSB), or the buffer control were used to treat N2 animals in the embryonic lethality assays. Total numbers of embryos scored: 1781, 805, 1249, 2645, 596, and 1862 embryos, from the left bar to the right bar in **a**; 2721, 2484, 880, and 743, from left to right in **b**; and 979, 875, 929, 939, 907, and 777, from left to right in **c**. Six independent assays (**a**, UV-Ctrl and UV-CM in **b**) and three independent assays (IR-Ctrl and IR-CM in **b, c**) were performed for each condition. Data are mean ± s.e.m. **P<0.01, ***P<0.001, "ns" is non-significant, two-sided, unpaired *t* test.
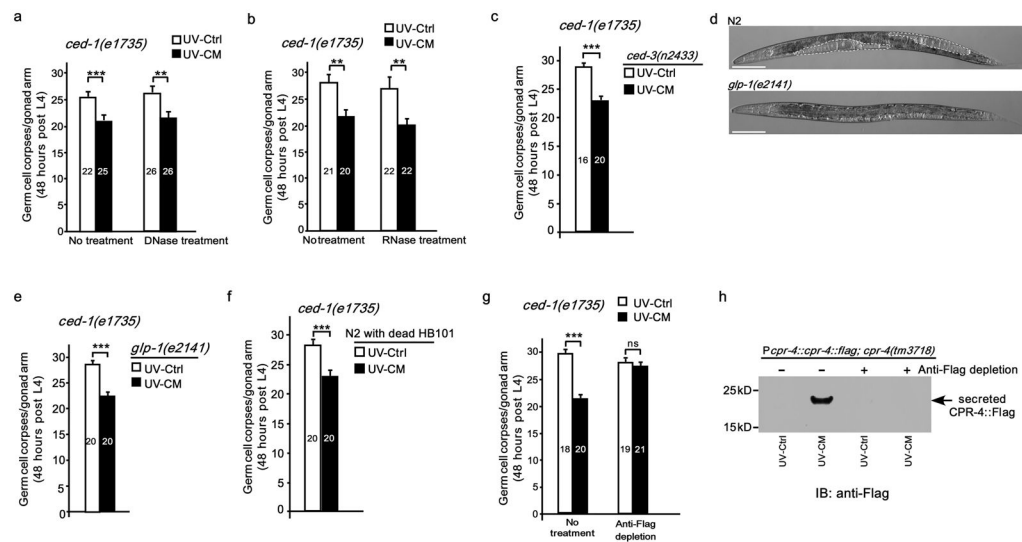
Extended Data Figure 2. Characterization of the nature and the source of the RIBE factors

a, b, Treatment of UV-CM and UV-Ctrl collected from N2 animals irradiated at 100 J/m^2 with RNase (1μg/μL) or DNase (0.01 Unit/μL) did not alter the apoptosis-inhibitory effect on *ced-1(e1735)* animals (Methods). Germ cell corpses were scored after 48-hour treatment of *ced-1(e1735)* L4 larvae. **c, e, f, g,** *ced-1(e1735)* L4 larvae were treated with UV-CM and UV-control (0.1 μg/μL) prepared from *ced-3(n2433)* animals (**c**), *glp-1(e2141ts)* animals grown at 25°C (**e**), N2 animals fed with formaldehyde-treated HB101 bacteria (**f**), and P*cpr-4::cpr-4::flag; cpr-4(tm3718)* animals with or without anti-Flag depletion (**g**), respectively. Data are mean ± s.e.m. The numbers of gonad arms scored are indicated inside the bars (**a–c, e–g**). ** *P* < 0.01, *** *P* <0.001, "ns", non-significant, two-sided, unpaired *t* test. **d**, Representative differential interference contrast (DIC) images (at least 10) of N2 and *glp-1(e2141)* adult animals grown at 25°C. The gonads of the N2 animal with multiple oocytes and fertilized eggs are outlined with dash lines. *glp-1(e2141)* animal had no visible germline. Scale bars indicate 100 μm. **h**, Immunoblotting analysis of secreted CPR-4::Flag in UV-CM and UV-Ctrl prepared from P*cpr-4::cpr-4::flag; cpr-4(tm3718)* animals with or without anti-Flag depletion treatment. For gel source data, see Supplementary Fig. 1.
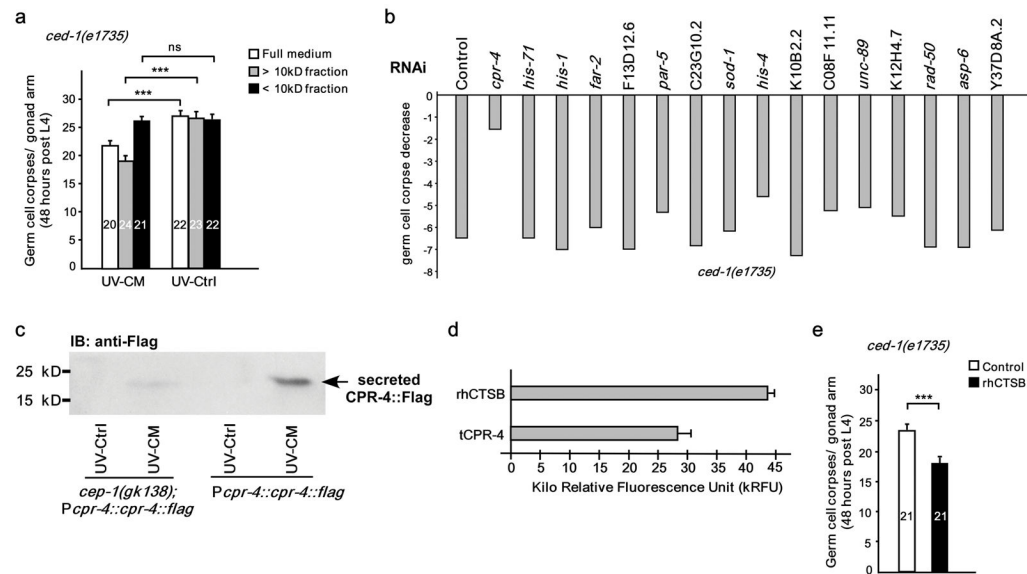
Extended Data Figure 3. Identification of CPR-4 as the RIBE factor

a, Full medium, >10 kD fraction, and <10 kD fraction of UV-CM and UV-Ctrl derived from N2 animals were used to treat *ced-1(e1735)* animals in germ cell corpse assays as in Fig. 1b. Data are mean ± s.e.m. The numbers of gonad arms scored are indicated inside the bars. **b,** Identification of CPR-4 as the RIBE factor through the RNAi screen. UV-Ctrl and UV-CM prepared from RNAi-treated animals were used to treat *ced-1(e1735)* animals. The number of germ cell corpse decrease (y axis) was calculated by subtracting the number of average germ cell corpses under UV-Ctrl treatment from that under UV-CM treatment. Among the candidate genes, RNAi of *eft-3*, *ubq-2* and *act-1* caused strong embryonic lethality and we were unable to obtain their UV-CM. RNAi of *his-1*, *his-4* and *his-71* caused partial embryonic lethality. 20 gonad arms were scored in each RNAi experiment. **c,** Secretion of CPR-4::Flag into UV-CM was greatly reduced in irradiated *cep-1(gk138)* animals carrying a single copy integration of P*cpr-4::cpr-4::flag* compared with that from irradiated N2 animals carrying the same P*cpr-4::cpr-4::flag* transgene. Concentrated UV-CM or UV-control (1 μg/ μL) from the indicated strains was subjected to the immunoblotting analysis using an antibody to the Flag epitope. **d,** The protease activity of 0.27 μM recombinant human Cathepsin B (rhCTSB) or 2.8 μM recombinant tCPR-4 protein was measured as in Fig. 2b. Data are mean ± s.e.m. (n= 6 in each assay). **e,** 0.27 μM of rhCTSB or the buffer control were used to treat *ced-1(e1735)* animals. Animals cultured in the rhCTSB buffer grew slower than in the tCPR-4 buffer and had less germ cell corpses. Data are mean ± s.e.m. (n= 21 in each assay). Germ cell corpses were scored after 48 hour treatment (**a, b, e**). *** *P* <0.001, "ns", non-significant, two-sided, unpaired *t* test (**a, e**). For gel source data, see Supplementary Fig. 1.

a

```
  1 MKYLILAALV AVTAGLVIPL VPKTQEAITE YVNSKQSLWK AEIPKDITIE QVKKRLMRTE
 61 FVAPHTPDVE VVKHDINEDT IPATFDARTQ WPNCMSINNI RDQSDCGSCW AFAAAEAASD
121 RFCIASNGAV NTLLSAEDVL SCCSNCGYGC EGGYPINAWK YLVKSGFCTG GSYEAQFGCK
181 PYSLAPCGET VGNVTWPSCP DDGYDTPACV NKCTNKNYNV AYTADKHFGS TAYAVGKKVS
241 QIQAEIIAHG PVEAAFTVYE DFYQYKTGVY VHTTGQELGG HAIRILGWGT DNGTPYWLVA
301 NSWNVNWGEN GYFRIIRGTN ECGIEHAVVG GVPKV
```

b

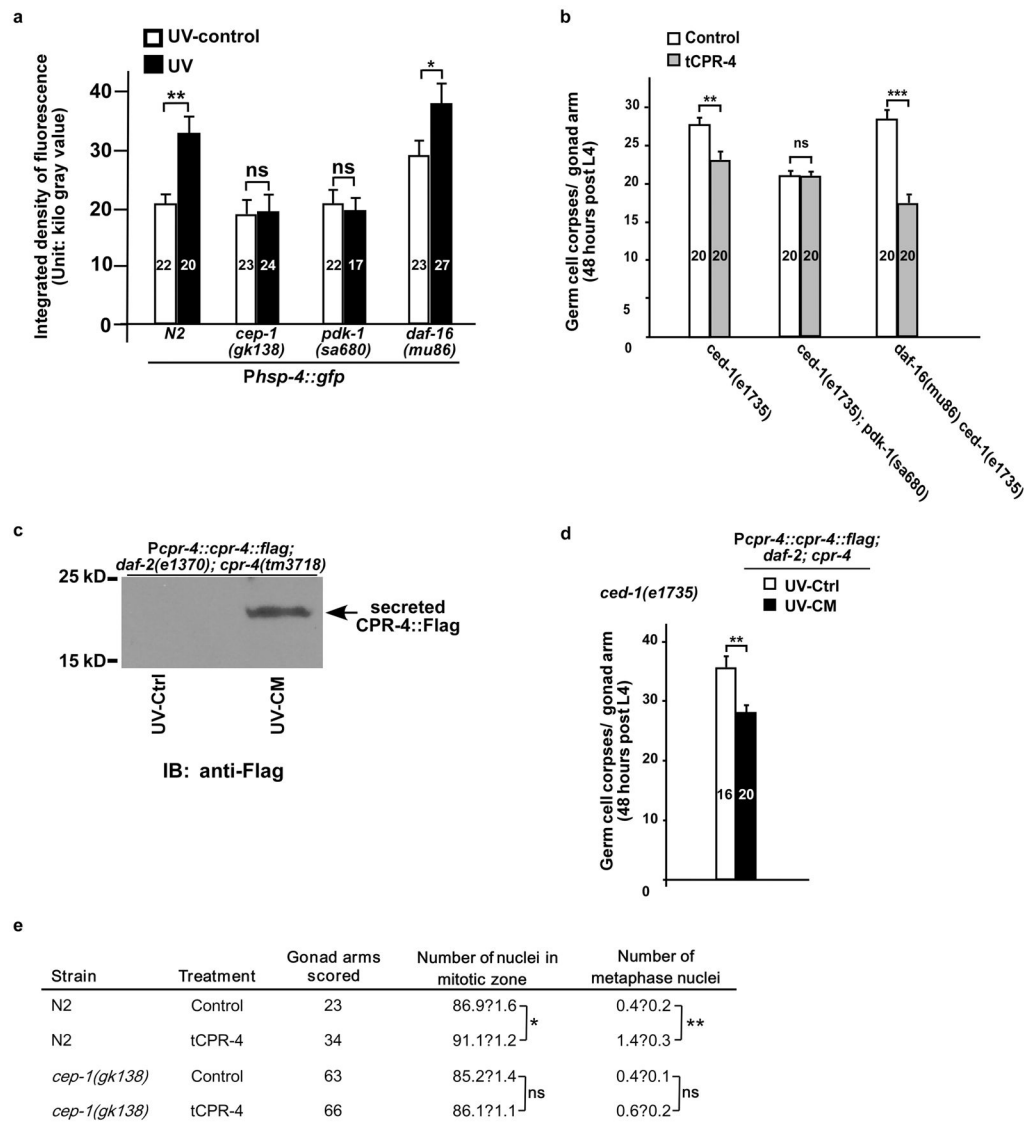Tryptic peptide: **HFGSTAYAVGK** Tryptic peptide: **GTNEcGIEHAVVGGVPK**

B	B Ions	B+2H	B-NH3	B-H2O	AA	Y Ions	Y+2H	Y-NH3	Y-H2O	Y
1	138.1	69.5			H	1,137.6	569.3	1,120.5	1,119.6	11
2	285.1	143.1			F	1,000.5	500.8	983.5	982.5	10
3	342.2	171.6			G	853.4	427.2	836.4	835.4	9
4	429.2	215.1		411.2	S	796.4	398.7	779.4	778.4	8
5	530.2	265.6		512.2	T	709.4	355.2	692.4	691.4	7
6	601.3	301.1		583.3	A	608.3	304.7	591.3		6
7	764.3	382.7		746.3	Y	537.3		520.3		5
8	835.4	418.2		817.4	A	374.2		357.2		4
9	934.4	467.7		916.4	V	303.2		286.2		3
10	991.5	496.2		973.5	G	204.1		187.1		2
11	1,137.6	569.3	1,120.5	1,119.6	K	147.1		130.1		1

B	B Ions	B+2H	B-NH3	B-H2O	AA	Y Ions	Y+2H	Y-NH3	Y-H2O	Y
1	58.0				G	1,723.8	862.4	1,706.8	1,705.8	17
2	159.1			141.1	T	1,666.8	833.9	1,649.8	1,648.8	16
3	273.1		256.1	255.1	N	1,565.8	783.4	1,548.7	1,547.8	15
4	402.2		385.1	384.2	E	1,451.7	726.4	1,434.7	1,433.7	14
5	562.2		545.2	544.2	C+57	1,322.7	661.8	1,305.7	1,304.7	13
6	619.2	310.1	602.2	601.2	G	1,162.7	581.8	1,145.6	1,144.6	12
7	732.3	366.7	715.3	714.3	I	1,105.6	553.3	1,088.6	1,087.6	11
8	861.3	431.2	844.3	843.3	E	992.6	496.8	975.5	974.5	10
9	998.4	499.7	981.4	980.4	H	863.5	432.3	846.5		9
10	1,069.4	535.2	1,052.4	1,051.4	A	726.5	363.7	709.4		8
11	1,168.5	584.8	1,151.5	1,150.5	V	655.4	328.2	638.4		7
12	1,267.6	634.3	1,250.5	1,249.6	V	556.3	278.7	539.3		6
13	1,324.6	662.8	1,307.6	1,306.6	G	457.3		440.3		5
14	1,381.6	691.3	1,364.6	1,363.6	G	400.3		383.2		4
15	1,480.7	740.8	1,463.7	1,462.7	V	343.2		326.2		3
16	1,577.7	789.4	1,560.7	1,559.7	P	244.2		227.1		2
17	1,723.8	862.4	1,706.8	1,705.8	K	147.1		130.1		1

Extended Data Figure 4. Representative MS/MS spectra from LTQ-Orbitrap used to confirm the identity of CPR-4 in UV-CM

a, Tryptic peptides of protein band 6 in the SDS PAGE gel (Fig. 1d) were analyzed by LC-MS/MS using LTQ-Orbitrap. The amino acid sequences of peptides identified by MS/MS analysis and matched to the amino acid sequences of CPR-4 are underlined and in Red. **b,** The MS/MS spectra of the two peptides identified in **a** are shown. The assignments of the fragmented ions observed to specific amino acid residues were performed using the Scaffold 3 search engine, and the search results are shown below the MS/MS spectra. The lower case "c" indicates the carbamidomethyl-modified cysteine residue in the tryptic peptide.
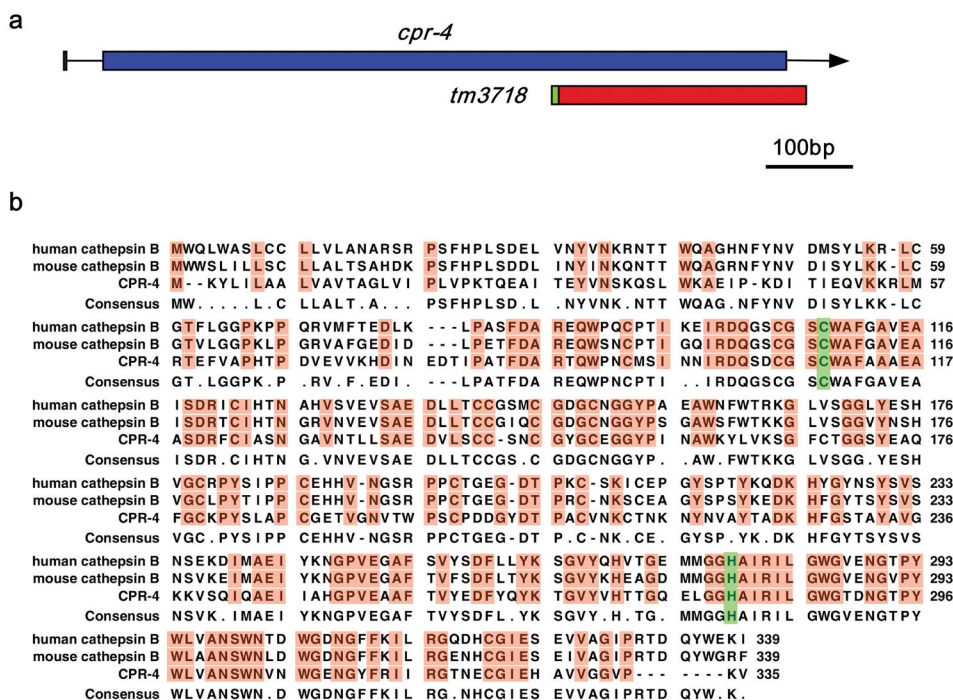
Extended Data Figure 5. The *cpr-4* deletion mutation and sequence alignment of human and mouse cathepsin B and CPR-4

a, A schematic representation of the *cpr-4* gene structure and the *tm3718* deletion. Exons are depicted as blue boxes and introns and the untranslated region as lines. The red box indicates the region of *cpr-4* removed by the 406 bp *tm3718* deletion. The green box indicates a 12 bp insertion. **b,** Sequence alignment of human cathepsin B, mouse cathepsin B, and CPR-4. Residues that are identical in all three proteins are shaded in pink. The two catalytic residues are shaded in green, which are the active-site Cysteine residue that serves as a nucleophile and the Histidine residue that acts as a general base to facilitate hydrolysis of the peptide bonds of the substrates[16], respectively.
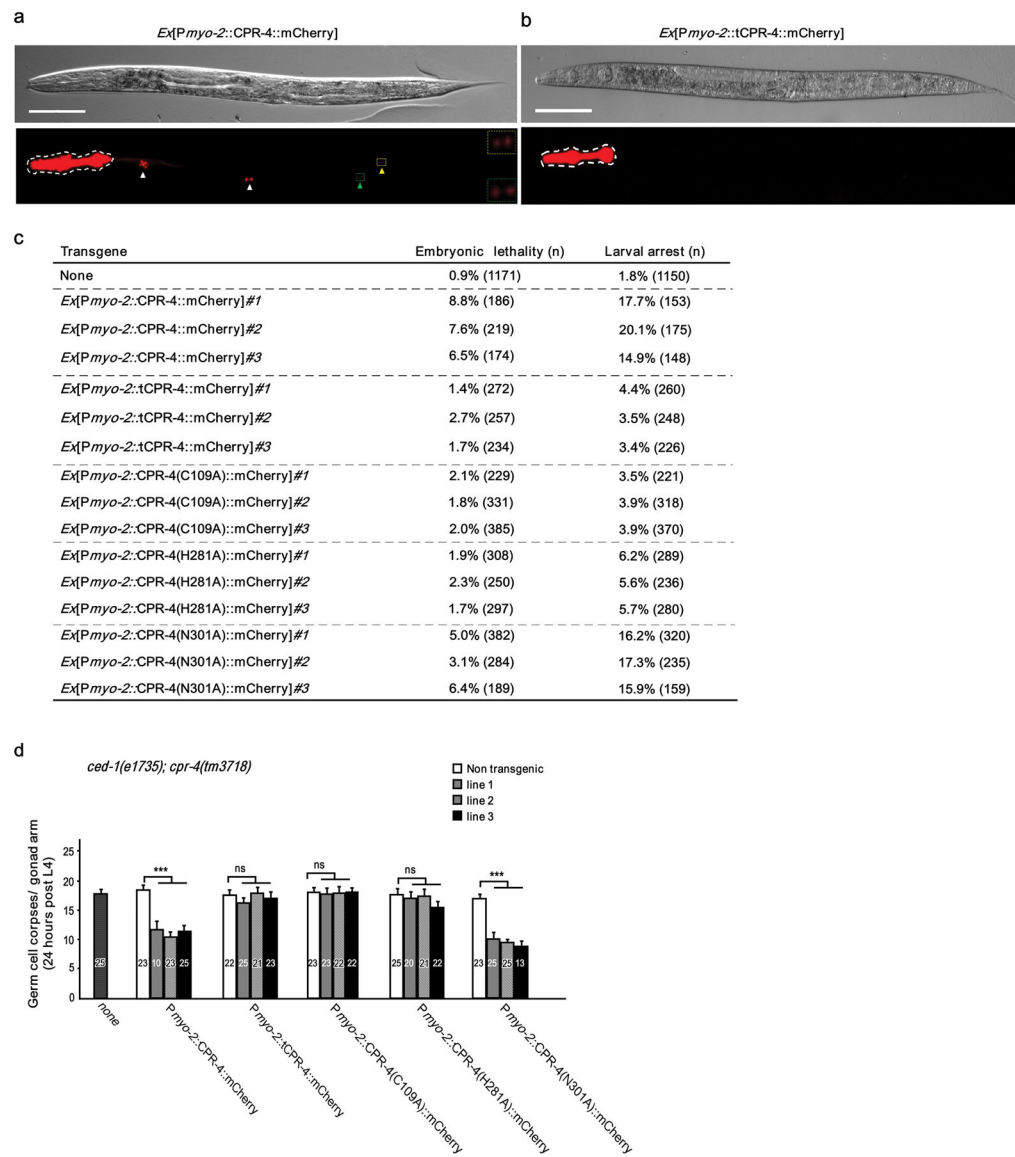
a, Localized UV irradiation assays. Animals of the indicated genotype were analyzed for the bystander P*hsp-4::gfp* response 24 hours post localized irradiation at the head region as described in Fig. 3. Data are mean ± s.e.m. The numbers of animals scored are indicated inside the bars.

Strain	Treatment	Gonad arms scored	Number of nuclei in mitotic zone	Number of metaphase nuclei
N2	Control	23	86.9?1.6	0.4?0.2
N2	tCPR-4	34	91.1?1.2	1.4?0.3
cep-1(gk138)	Control	63	85.2?1.4	0.4?0.1
cep-1(gk138)	tCPR-4	66	86.1?1.1	0.6?0.2

Extended Data Figure 6. Analysis of the roles of additional genes in mediating RIBE
a, Localized UV irradiation assays. Animals of the indicated genotype were analyzed for the bystander P*hsp-4::gfp* response 24 hours post localized irradiation at the head region as described in Fig. 3. Data are mean ± s.e.m. The numbers of animals scored are indicated inside the bars. **b,** Germ cell corpse assays after tCPR-4 treatment. 2.8 μM recombinant tCPR-4 protein or buffer control was used to treat L4 larvae of the indicated genotype as described in Fig. 4a. Data are mean ± s.e.m. The numbers of gonad arms scored are indicated inside the bars. **c**, Immunoblotting analysis of secreted CPR-4::Flag in UV-CM and UV-Ctrl from P*cpr-4::cpr-4::flag; daf-2(e1730); cpr-4(tm3718)* animals was done as in Fig. 1f. d, Germ cell corpse assays. *ced-1(e1735)* L4 larvae were treated with UV-CM and UV-control (0.1 μg/μL) prepared from **c**. Data are mean ± s.e.m. The numbers of gonad arms scored are indicated inside the bars. **e**, Germ cell proliferation assays. N2 and *cep-1(gk138)* L4 larvae were treated in S-Medium containing 2.8 μM of recombinant tCPR-4 or buffer control for 48 hours. The numbers of nuclei and metaphase nuclei in the mitotic zone of the

germline were scored (Methods). Data are mean ± s.e.m. In **a, b, d, e**, * $P<0.05$, ** $P< 0.01$, *** $P< 0.001$, "ns", non-significant, two-sided, unpaired t test. For gel source data, see Supplementary Fig. 1.
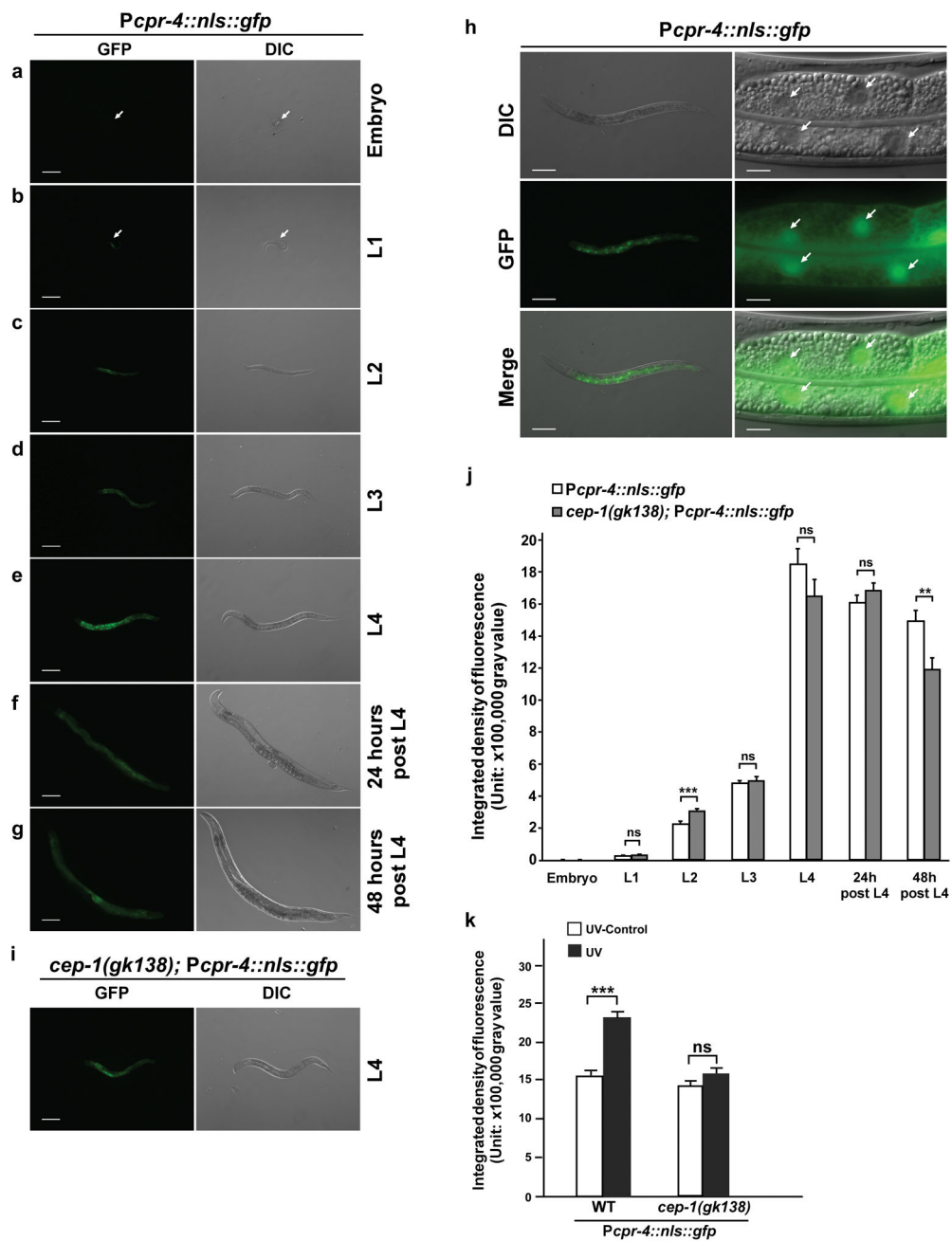
Extended Data Figure 7. The expression patterns of *cpr-4* in *C. elegans*
a–g, i, Representative GFP and DIC images (at least 15 each) of N2 animals (**a–g**) or *cep-1(gk138)* animals (**i**) carrying a single-copy integration of P*cpr-4::nls::gfp* at the indicated developmental stages. Arrows point to the embryo and the L1 larva that showed no or very dim GFP (**a, b**). Scale bar, 100 μm. **h,** Representative DIC, GFP, and DIC/GFP

merged images (at least 15) of a L4 larva carrying the same P*cpr-4::nls::gfp* transgene (left column) and corresponding 10-fold magnified images showing GFP expression in intestinal cells (right column). GFP was seen mostly in the nuclei (indicated by arrows). Scale bars, 100 μm (left) and 10 μm (right), respectively. **j,** The intensity of GFP fluorescence in P*cpr-4::nls::gfp* and *cep-1(gk138);* P*cpr-4::nls::gfp* animals at different developmental stages was quantified using the Image J software. Data are mean ± s.e.m. n= 28, 28, 24, 31, 30, 33, 52, 52, 19, 28, 52, 52, 24, and 25 animals scored, from the left bar to the right bar, respectively. The significance of difference between two different strains at the same developmental stage was determined by two-sided, unpaired *t* test. ** $P < 0.01$, ***$P < 0.001$, "ns", non-significant. **k**, Quantification of GFP intensity in N2 and *cep-1(gk138)* animals carrying the same single-copy P*cpr-4::nls::gfp* transgene irradiated by UV or sham-irradiated using Image J. Data are mean ± s.e.m. n= 38, 37, 32, and 30 animals scored, from the left bar to the right bar, respectively. The significance of difference between different conditions was determined by two-sided, unpaired *t* test. *** $P < 0.001$, "ns", non-significant.

a, *Ex[Pmyo-2::CPR-4::mCherry]*   **b**, *Ex[Pmyo-2::tCPR-4::mCherry]*

c

Transgene	Embryonic lethality (n)	Larval arrest (n)
None	0.9% (1171)	1.8% (1150)
Ex[Pmyo-2::CPR-4::mCherry]#1	8.8% (186)	17.7% (153)
Ex[Pmyo-2::CPR-4::mCherry]#2	7.6% (219)	20.1% (175)
Ex[Pmyo-2::CPR-4::mCherry]#3	6.5% (174)	14.9% (148)
Ex[Pmyo-2::tCPR-4::mCherry]#1	1.4% (272)	4.4% (260)
Ex[Pmyo-2::tCPR-4::mCherry]#2	2.7% (257)	3.5% (248)
Ex[Pmyo-2::tCPR-4::mCherry]#3	1.7% (234)	3.4% (226)
Ex[Pmyo-2::CPR-4(C109A)::mCherry]#1	2.1% (229)	3.5% (221)
Ex[Pmyo-2::CPR-4(C109A)::mCherry]#2	1.8% (331)	3.9% (318)
Ex[Pmyo-2::CPR-4(C109A)::mCherry]#3	2.0% (385)	3.9% (370)
Ex[Pmyo-2::CPR-4(H281A)::mCherry]#1	1.9% (308)	6.2% (289)
Ex[Pmyo-2::CPR-4(H281A)::mCherry]#2	2.3% (250)	5.6% (236)
Ex[Pmyo-2::CPR-4(H281A)::mCherry]#3	1.7% (297)	5.7% (280)
Ex[Pmyo-2::CPR-4(N301A)::mCherry]#1	5.0% (382)	16.2% (320)
Ex[Pmyo-2::CPR-4(N301A)::mCherry]#2	3.1% (284)	17.3% (235)
Ex[Pmyo-2::CPR-4(N301A)::mCherry]#3	6.4% (189)	15.9% (159)

d

Extended Data Figure 8. Pharyngeal expression of CPR-4 results in embryonic lethality, larval arrest, and reduced germ cell death

a, **b,** Representative DIC and mCherry images (at least 10) of adult animals with pharyngeal expression of CPR-4::mCherry (**a**) and tCPR-4::mCherry (**b**). White dash lines highlight the edge of the pharynx. Arrowheads indicate cells, including coelomocytes, that had taken up CPR-4::mCherry (**a**), which was made in and secreted from the pharynx and transported to other parts of the animal, probably through the pseudocoelom, a fluid-filled body cavity. The enlarged images of two pairs of posterior cells with weak fluorescence (indicated by color arrowheads) are shown in dash boxes with corresponding colors. Scale bars, 100 μm. **c,** The percentages of embryonic lethality and larval arrest were scored in embryos or larvae carrying Pmyo-2::CPR-4::mCherry (wild-type or mutant) or Pmyo-2::tCPR-4::mCherry transgenes. Three independent transgenic lines were scored for each construct. The number of newly hatched transgenic L1 larvae scored and the number of transgenic embryos scored

are indicated in parentheses. The increased larval arrest seen in P*myo-2*::CPR-4::mCherry transgenic animals was blocked when transgenic animals were treated with *cpr-4* RNAi (Extended Data Table 2), indicating that reducing *cpr-4* expression prevents larval arrest. All animals carry the *ced-1(e1735)* and *cpr–4(tm3718)* mutations (**a–c**). **d,** Quantification of germ cell corpses in transgenic animals. L4 *ced-1(e1735); cpr-4(tm3718)* animals carrying the indicated transgenes were grown on regular NGM plates for 24 hours before examination. Data are mean ± s.e.m. The numbers of gonad arms scored are indicated inside the bars. The significance of difference between transgenic and non-transgenic animals was determined by one-way analysis of variance (ANOVA). *** $P < 0.001$, "ns", non-significant.

Extended Data Table 1

A summary of peptide identification information in bands 1–10 by LC-MS/MS analysis using LTQ-Orbitrap.

Band No.	Protein name	Gene name	Protein ID probability	No. of unique peptides	Percentage of sequence coverage
1	Not determined				
2	Putative serine protease K12H4.7	K12H4.7	99.80%	2	5.29%
	Elongation factor 1-alpha	*eft-3*	99.80%	2	4.10%
3	Putative serine protease K12H4.7	K12H4.7	100.00%	3	7.65%
	Putative phospholipase B-like 1	Y37D8A.2	100.00%	2	5.78%
4	Aspartic protease 6	*asp-6*	100.00%	4	19.00%
5	Cathepsin B-like cysteine proteinase 4	*cpr-4*	100.00%	3	11.30%
	Muscle M-line assembly protein unc-89	*unc-89*	99.90%	2	0.24%
	Uncharacterized serine carboxypeptidase F13S12.6	F13D12.6	99.80%	2	4.41%
	Aspartic protease 6	*asp-6*	99.80%	2	10.80%
6	Aspartic protease 6	*asp-6*	100.00%	6	19.00%
	Uncharacterized serine carboxypeptidase K10B2.2	K10B2.2	100.00%	3	7.66%
	DNA repair protein rad-50	*rad-50*	99.80%	2	0.92%
	Cathepsin B-like cysteine proteinase 4	*cpr-4*	99.80%	2	8.36%
7	Actin-1	*act-1*	100.00%	7	18.40%
	Histone H4	*his-1*	100.00%	5	41.70%
	Elongation factor 1-alpha	*eft-3*	100.00%	3	6.26%
	Superoxide dismutase [Cu-Zn]	*sod-1*	100.00%	3	23.30%
	14-3-3-like protein 1	*par-5*	99.80%	2	7.26%
	Histone H3.3 type 1	*his-71*	100.00%	2	10.30%
	Ubiquitin-60S ribosomal protein L40	*ubq-2*	99.80%	2	11.70%
	Histone H2B 2	*his-4*	99.80%	2	13.00%

Band No.	Protein name	Gene name	Protein ID probability	No. of unique peptides	Percentage of sequence coverage
8	Uncharacterized serine carboxypeptidase F13S12.6	F13D12.6	100.00%	5	10.40%
	Fatty-acid and retinol-binding protein 2	*far-2*	100.00%	3	17.00%
	UPF0375 protein C08F11.11	C08F11.11	100.00%	3	36.00%
	Actin-1	*act-1*	99.90%	2	7.45%
	RutC family protein C23G10.2	C23G10.2	99.80%	2	13.50%
9	Aspartic protease 6	*asp-6*	100.00%	3	11.60%
	Uncharacterized serine carboxypeptidase F13S12.6	F13D12.6	99.70%	2	4.85%
	Cathepsin B-like cysteine proteinase 4	*cpr-4*	99.70%	2	8.36%
10	Aspartic protease 6	*asp-6*	100.00%	4	9.77%
	Uncharacterized serine carboxypeptidase F13S12.6	F13D12.6	99.80%	2	4.85%
	Cathepsin B-like cysteine proteinase 4	*cpr-4*	99.80%	2	10.40%
	Histone H4	*his-1*	99.80%	2	17.50%

Extended Data Table 2

cpr-4 RNAi treatment of P*myo-2*::CPR-4::mCherry transgenic animals. All strains contain the *ced-1(e1735)* and *cpr-4(tm3718)* mutations. RNAi experiments were carried out using a bacteria-feeding protocol[40]. Larval arrest was scored as described in Methods.

Genotype	Larval arrest (%)	n
Control RNAi	0%	150
cpr-4 RNAi	0%	150
Ex[P*myo*-2::CPR-4::mCherry]#*1*; Control RNAi	9%	135
Ex[P*myo*-2::CPR-4::mCherry]#2; Control RNAi	7%	172
Ex[P*myo*-2::CPR-4::mCherry] #*1*; *cpr-4* RNAi	1%	136
Ex[P*myo*-2::CPR-4::mCherry] #*2*; *cpr-4* RNAi	1%	163

Supplementary Material

Refer to Web version on PubMed Central for supplementary material.

Acknowledgments

References

1. Mothersill C, Seymour C. Radiation-induced bystander effects: past history and future directions. Radiat Res. 2001; 155:759–767. [PubMed: 11352757]

2. Prise KM, O'Sullivan JM. Radiation-induced bystander signalling in cancer therapy. Nat Rev Cancer. 2009; 9:351–360. [PubMed: 19377507]

3. Rzeszowska-Wolny J, Przybyszewski WM, Widel M. Ionizing radiation-induced bystander effects, potential targets for modulation of radiotherapy. Eur J Pharmacol. 2009; 625:156–164. [PubMed: 19835860]

4. Stergiou L, Doukoumetzidis K, Sendoel A, Hengartner MO. The nucleotide excision repair pathway is required for UV-C-induced apoptosis in *Caenorhabditis elegans*. Cell Death Differ. 2007; 14:1129–1138. [PubMed: 17347667]

5. Derry WB, Putzke AP, Rothman JH. *Caenorhabditis elegans* p53: Role in apoptosis, meiosis, and stress resistance. Science. 2001; 294:591–595. [PubMed: 11557844]

6. Schumacher B, Hofmann K, Boulton S, Gartner A. The C. elegans homolog of the p53 tumor suppressor is required for DNA damage-induced apoptosis. Curr Biol. 2001; 11:1722–1727. [PubMed: 11696333]

7. Klokov D, et al. Low dose IR-induced IGF-1-sCLU expression: a p53-repressed expression cascade that interferes with TGFbeta1 signaling to confer a pro-survival bystander effect. Oncogene. 2013; 32:479–490. [PubMed: 22391565]

8. Koturbash I, et al. In vivo bystander effect: Cranial X-irradiation leads to elevated DNA damage, altered cellular proliferation and apoptosis, and increased p53 levels in shielded spleen. Int J Radiat Oncol Biol Phys. 2008; 70:554–562. [PubMed: 18207032]

9. Sun Y, et al. Treatment-induced damage to the tumor microenvironment promotes prostate cancer therapy resistance through WNT16B. Nat Med. 2012; 18:1359–1368. [PubMed: 22863786]

10. Buck MR, Karustis DG, Day NA, Honn KV, Sloane BF. Degradation of Extracellular-Matrix Proteins by Human Cathepsin-B from Normal and Tumor-Tissues. Biochem J. 1992; 282:273–278. [PubMed: 1540143]

11. Poole AR, Tiltman KJ, Recklies AD, Stoker TA. Differences in secretion of the proteinase cathepsin B at the edges of human breast carcinomas and fibroadenomas. Nature. 1978; 273:545–547. [PubMed: 661963]

12. Larminie CG, Johnstone IL. Isolation and characterization of four developmentally regulated cathepsin B-like cysteine protease genes from the nematode *Caenorhabditis elegans*. DNA Cell Biol. 1996; 15:75–82. [PubMed: 8561899]

13. Lorimore SA, Rastogi S, Mukherjee D, Coates PJ, Wright EG. The influence of p53 functions on radiation-induced inflammatory bystander-type signaling in murine bone marrow. Radiat Res. 2013; 179:406–415. [PubMed: 23578188]

14. Calfon M, et al. IRE1 couples endoplasmic reticulum load to secretory capacity by processing the XBP-1 mRNA. Nature. 2002; 415:92–96. [PubMed: 11780124]

15. Bertucci A, Pocock RD, Randers-Pehrson G, Brenner DJ. Microbeam irradiation of the C. elegans nematode. J Radiat Res. 2009; 50(Suppl A):A49–54. [PubMed: 19346684]

16. Mort JS, Buttle DJ. Cathepsin B. Int J Biochem Cell Biol. 1997; 29:715–720. [PubMed: 9251238]

17. Shore DE, Ruvkun G. A cytoprotective perspective on longevity regulation. Trends Cell Biol. 2013; 23:409–420. [PubMed: 23726168]

18. Kenyon CJ. The genetics of ageing. Nature. 2010; 464:504–512. [PubMed: 20336132]

19. Perrin AJ, et al. Noncanonical control of C. elegans germline apoptosis by the insulin/IGF-1 and Ras/MAPK signaling pathways. Cell Death Differ. 2013; 20:97–107. [PubMed: 22935616]

20. Scott BA, Avidan MS, Crowder CM. Regulation of hypoxic death in C. elegans by the insulin/IGF receptor homolog DAF-2. Science. 2002; 296:2388–2391. [PubMed: 12065745]

21. Paradis S, Ailion M, Toker A, Thomas JH, Ruvkun G. A PDK1 homolog is necessary and sufficient to transduce AGE-1 PI3 kinase signals that regulate diapause in *Caenorhabditis elegans*. Genes Dev. 1999; 13:1438–1452. [PubMed: 10364160]

22. Lin K, Dorman JB, Rodan A, Kenyon C. daf-16: An HNF-3/forkhead family member that can function to double the life-span of *Caenorhabditis elegans*. Science. 1997; 278:1319–1322. [PubMed: 9360933]

23. Ogg S, et al. The Fork head transcription factor DAF-16 transduces insulin-like metabolic and longevity signals in C. elegans. Nature. 1997; 389:994–999. [PubMed: 9353126]

24. Michaelson D, Korta DZ, Capua Y, Hubbard EJ. Insulin signaling promotes germline proliferation in C. elegans. Development. 2010; 137:671–680. [PubMed: 20110332]

25. Pinkston JM, Garigan D, Hansen M, Kenyon C. Mutations that increase the life span of C. elegans inhibit tumor growth. Science. 2006; 313:971–975. [PubMed: 16917064]

26. Nikjoo H, Khvostunov IK. A theoretical approach to the role and critical issues associated with bystander effect in risk estimation. Hum Exp Toxicol. 2004; 23:81–86. [PubMed: 15070065]

27. Mothersill C, Seymour C. Radiation-induced bystander and other non-targeted effects: novel intervention points in cancer therapy? Curr Cancer Drug Targets. 2006; 6:447–454. [PubMed: 16918311]

28. Recklies AD, Tiltman KJ, Stoker TA, Poole AR. Secretion of proteinases from malignant and nonmalignant human breast tissue. Cancer Res. 1980; 40:550–556. [PubMed: 6258782]

29. Barrett AJ, Kirschke H, Cathepsin B, Cathepsin H, cathepsin L. Methods Enzymol. 1981; 80(Pt C): 535–561. [PubMed: 7043200]

30. Shree T, et al. Macrophages and cathepsin proteases blunt chemotherapeutic response in breast cancer. Genes Dev. 2011; 25:2465–2479. [PubMed: 22156207]

31. Brenner S. The genetics of *Caenorhabditis elegans*. Genetics. 1974; 77:71–94. [PubMed: 4366476]

32. Frokjaer-Jensen C, et al. Single-copy insertion of transgenes in *Caenorhabditis elegans*. Nat Genet. 2008; 40:1375–1383. [PubMed: 18953339]

33. Timmons L, Court DL, Fire A. Ingestion of bacterially expressed dsRNAs can produce specific and potent genetic interference in *Caenorhabditis elegans*. Gene. 2001; 263:103–112. [PubMed: 11223248]

34. Pepper ASR, Killian DJ, Hubbard EJA. Genetic analysis of *Caenorhabditis elegans* glp-1 mutants suggests receptor interaction or competition. Genetics. 2003; 163:115–132. [PubMed: 12586701]

35. Bendtsen JD, Nielsen H, von Heijne G, Brunak S. Improved prediction of signal peptides: SignalP 3.0. J Mol Biol. 2004; 340:783–795. [PubMed: 15223320]

36. Mello CC, Kramer JM, Stinchcomb D, Ambros V. Efficient Gene-Transfer in C-Elegans - Extrachromosomal Maintenance and Integration of Transforming Sequences. EMBO J. 1991; 10:3959–3970. [PubMed: 1935914]

37. Gu T, Orita S, Han M. *Caenorhabditis elegans* SUR-5, a novel but conserved protein, negatively regulates LET-60 Ras activity during vulval induction. Mol Cell Biol. 1998; 18:4556–4564. [PubMed: 9671465]

38. Paquet C, Sane AT, Beauchemin M, Bertrand R. Caspase- and mitochondrial dysfunction-dependent mechanisms of lysosomal leakage and cathepsin B activation in DNA damage-induced apoptosis. Leukemia. 2005; 19:784–791. [PubMed: 15759029]

39. Hoogewijs D, Houthoofd K, Matthijssens F, Vandesompele J, Vanfleteren JR. Selection and validation of a set of reliable reference genes for quantitative sod gene expression analysis in C. elegans. BMC Mol Biol. 2008; 9:9. [PubMed: 18211699]

40. Timmons L, Court DL, Fire A. Ingestion of bacterially expressed dsRNAs can produce specific and potent genetic interference in *Caenorhabditis elegans*. Gene. 2001; 263:103–112. [PubMed: 11223248]
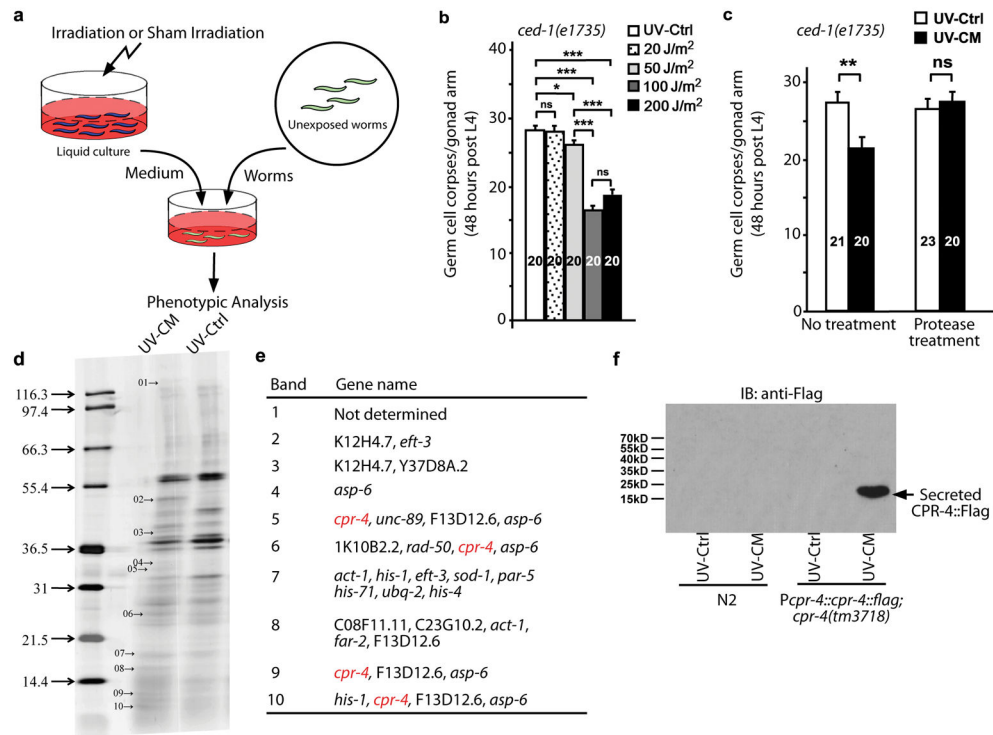
Figure 1. Identification of the RIBE factor

a, Schematic presentation of the RIBE assay in *C. elegans* (Methods). **b, c,** *ced-1(e1735)* L4 larvae were cultured in UV-CM from N2 animals irradiated at the indicated dosage (**b**) or UV-CM (100 J/m^2) treated with Trypsin protease (50 ng/μL)(**c**). Germ cell corpses were scored after 48 hours. Data are mean ± s.e.m. The numbers of gonad arms scored are indicated inside the bars. * $P<0.05$, ** $P<0.01$, *** $P<0.001$, "ns", non-significant, two-sided, unpaired *t* test. **d, e,** Mass spectrometry analysis. Concentrated >10 kD UV-CM and UV-Ctrl fractions were resolved on SDS polyacrylamide gel (PAGE) and silver stained (**d**). Protein identities in bands unique to UV-CM (marked by numbers) are shown (**e**). **f**, CPR-4::Flag was secreted into UV-CM from P*cpr-4::cpr-4::flag* animals. UV-CM and UV-Ctrl (1 μg/μL) were resolved on SDS PAGE and detected by immunoblotting (IB). For gel source data, see Supplementary Fig. 1.
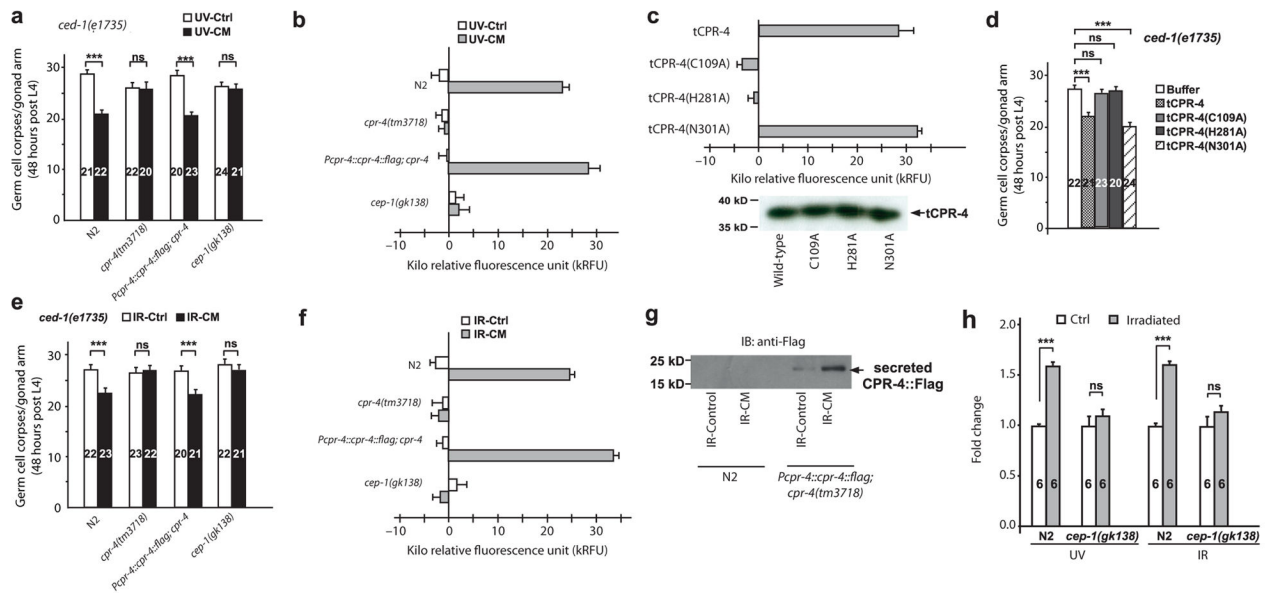
Figure 2. CPR-4 is a RIBE factor

a, d, e, Conditioned medium (0.1 μg/μL) from the indicated strains (**a, e**) or 2.8 μM of recombinant tCPR-4 proteins (**d**) were used to treat *ced-1(e1735)* animals as in Fig. 1b. **b, c, f,** Protease activity of conditioned medium (0.1 μg/μL) from the indicated strains (**b, f**) or 2.8 μM tCPR-4 proteins (**c**). Immunoblotting image of tCPR-4 proteins is below **c. g,** CPR-4::Flag was secreted into IR-CM from P*cpr-4::cpr-4::flag* animals. IR-CM and IR-Ctrl (1 μg/μL) resolved on SDS PAGE were detected by immunoblotting. **h,** Relative *cpr-4* mRNA levels (fold change) in the indicated strains were determined by quantitative RT-PCR, compared to those of sham-irradiated samples (Ctrl). Data are mean ± s.e.m. (**a–f, h**). The numbers of gonad arms scored are indicated inside the bars (**a, d, e**) and n=6 in each group for other assays (**b, c, f, h**); *** $P<0.001$, "ns", non-significant, two-sided, unpaired t test (**a, d, e, h**). For gel source data, see Supplementary Fig. 1.
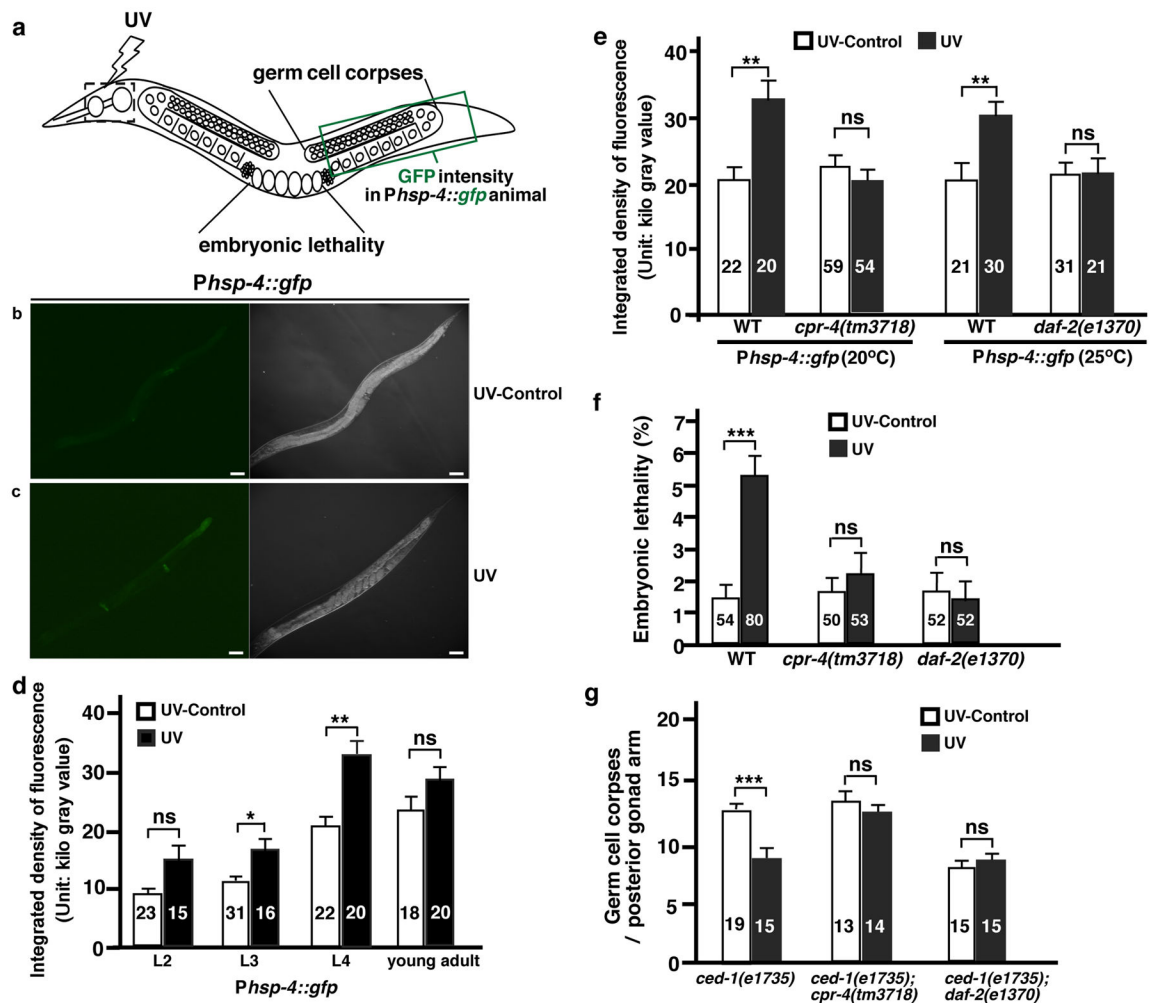
Figure 3. CPR-4 and DAF-2 mediate RIBE in a localized UV irradiation (LUI) model
a, Schematic presentation of an intra-animal model to assay RIBE. The pharyngeal area of the animal was irradiated and RIBE were analyzed in three unexposed areas as indicated (Methods). **b, c,** Representative images (at least 20) of P*hsp-4::gfp* animals with or without LUI. Animal tails to the upper right. Scale bars, 50 μm. **d,** Assays of the P*hsp-4::gfp* response to LUI at different developmental stages. **e-g,** The indicated strains were analyzed for the P*hsp-4::gfp* response (**e**), F1 embryonic lethality (**f**), and germ cell corpses in posterior gonads (**g**) 24 hours post LUI. Some experiments in **e** and all in **f** were done at 25°C. Data are mean ± s.e.m. The numbers of animals (**d, e**), plates with embryos (**f**), or gonad arms (**g**) scored are indicated inside the bars. * $P<0.05$, ** $P<0.01$, *** $P<0.001$, "ns", non-significant, two-sided, unpaired t test (**d–g**).
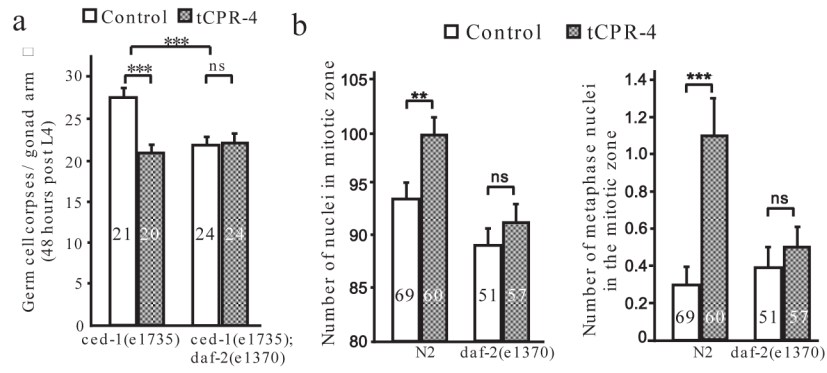
Figure 4. CPR-4 acts through DAF-2 to exert RIBE

a, b, L4 larvae of the indicated strains were treated with 2.8 μM of tCPR-4 or buffer control for 48 hours. Data are mean ± s.e.m. The numbers of gonad arms scored are indicated inside the bars. ** $P<0.01$, *** $P<0.001$, "ns", non-significant, two-sided, unpaired t test.